2022

Epitrochoidal Gerotor Profiles with Asymmetric Lobes

Matthew Read

Epitrochoidal Gerotor Profiles with Asymmetric Lobes

Matthew READ

Department of Mechanical Engineering and Aeronautics,
City, University of London
London, UK
Email: m.read@city.ac.uk

ABSTRACT

Gerotor pumps operate with two rotors each rotating in the same direction about parallel but offset axes. Commerical applications for these machines include oil pumps, fuel pumps and hydraulic power transmission. It is also possible to use the gerotor configuration to achieve internal compression by specifying appropriate discharge port geometry, and the addition of helical twist to the rotors has been shown to achieve further benefits of reducing porting losses and power transfer between rotors. In either pump or compressor configuration, a motor drives the externally geared inner rotor. This meshes with the internally geared outer rotor to form a number of separate working chambers. These conjugate rotor profiles can be generated by a range of methods. Each rotor profile must have rotational symmetry, with a repeating lobe profile. These lobe profiles generally also have reflective symmetry about a radial line passing through the lobe tip, and the optimisation of this lobe geometry has been shown to be an important factor in machine performance. It is however possible to generate asymmetric lobe profiles for gerotor machines, allowing further optimisation and improved performance. This paper describes how pin-generated epitrochoidal asymmetric lobe profiles can be defined, establishes the geometric constraints, and characterises the influence of geometry on some key performance parameters in order to investigate the potential benefits of asymmetric lobes.

1. INTRODUCTION

The concept of internally geared positive displacement machines was introduced in a patent by Moineau (1934). In this configuration, rotors are shaped such that an externally lobed inner rotor meshes with an internally lobed outer rotor, with a number of continuous points of contact occurring between the rotors that delineate separate working chambers. Once appropriate axial ports in the casing are created to allow suction and discharge of the fluid, the changing area of these working chambers results in a mechanism able to operate as a positive displacement machine. This type of machine is commonly used for pumping oil and fuel, and as hydraulic pumps and motors.

More recently, there has been renewed interest in the concept of using gerotor profiles with helical rotors to achieve an internally geared screw compressor. A concept involving a constant rotor profile and helix lead has previously been described (Read et al., 2020, 2022). This configuration features fixed port plates at the suction and discharge end faces that allow control of the periods when fluid is able to enter and leave a working chamber. This configuration has potential advantages over existing compressors relating to reduced leakage areas, reduced drag losses, and codirectional thermal expansion. As with conventional twin screw compressors, the swept volume and contact forces between rotors are key design parameters for the internally geared configuration, and the rotor profiles have been shown to have a strong influence on this.

Significant research has been directed at generating appropriate rotor profiles for these 'gerotor' machine applications, and characterizing the influence of geometrical parameters and operating conditions on machine performance. Some key literature relating to rotor profile generation includes the work of Colborne (1974) and Beard et al (1992, 1992) on the characterization of epi & hypotrochoidal profiles for pumping applications. Litvin and Feng (1996) and Vecchiato et al. (2001) applied gearing theory to determine the necessary condition to avoid undercutting in cycloidal profiles. A number of papers by Hsieh (2007, 2009, 2012) have considered rotor profiles generated using various types of cycloid and trochoid, and investigated the resulting pump performance. A wide range of analysis methods have been used to investigate the performance of gerotor pumps, as described in the comprehensive review conducted

by Rundo (2017). More recently, Jacazio et al. (2019) have considered the generation of asymmetric rotor profiles using a generating pin formed from two elliptical curve sections with a common center. Multi-objective optimisation of the rotor geometry is then performed, demonstrating that asymmetric profiles can potentially achieve minor performance improvements over symmetric profiles (hence referred to as 'second-order' optimisation) for a pump application. This paper introduces an alternative method for generating asymmetric rotor profiles based on the commonly used circular pin geometry. The method for generating conventional profiles is reviewed, before the requirements for asymmetric profiles are introduced. Examples of this new type of asymmetric profile are shown, and the potential influence on machine operation and performance are discussed.

2. DESCRIPTION OF CIRCULAR PIN-GENERATED ROTOR PROFILES

Internal pin-generated gearing can be used to generate meshing rotor profiles. Continuous contact points are achieved when the inner gear contains one less or one more lobe than the outer gear. It is possible to generate two types of cycloidal gearing in this way;

1. An extended epicycloid profile is generated on the gear with the smaller centrode when the profile of the gear with larger centrode is partially defined by a circular pin,
2. An extended hypocycloid profile is generated on the gear with the larger centrode when the profile of the gear with smaller centrode is partially defined by a circular pin.

The geometry and position of the pins on a rotor consisting of N_1 lobes can be defined in the coordinate system S_1 as shown in Figure 1. By rotating this profile in the coordinate system of a second rotor, S_2, with a parallel but non-coincident axis and $N_2 = N_1 \pm 1$ lobes, the profile of this second rotor, Ψ_2, can be found by application of the meshing equation. The geometry used to generate the rotor profiles is illustrated in Figure 1 for the case when $N_1 > N_2$. This result also allows Ψ_{1p}, the section of rotor profile Ψ_1 defined by the circular arc of the pin (i.e. when $\theta_{min} \leq \theta \leq \theta_{max}$) to be defined. Rotation of Ψ_2 in coordinate system S_1 then generates the conjugate profile (or fillet), Ψ_{1q}, that connects the sections of circular profile in order create a complete rotor profile, Ψ_1, that achieves multiple points of continuous contact with Ψ_2. Alternatively, a non-conjugate fillet section can be defined for Ψ_{1q}; it is clear that any arbitrary profile can be defined as long as it does not infringe on the conjugate profile, which would result in interference between the rotors. While this may simplify manufacturing of the rotors, it results in a non-zero minimum area for the working chambers formed. For machines using helical rotor profiles, it has been shown that a conjugate fillet profile is necessary in order to prevent direct leakage paths between working chambers (Read, 2020). For applications with straight rotors, such as gerotor pumps, the fillet profile is often close to the conjugate profile in order to limit the minimum volume. All profiles considered in this paper are fully conjugate.

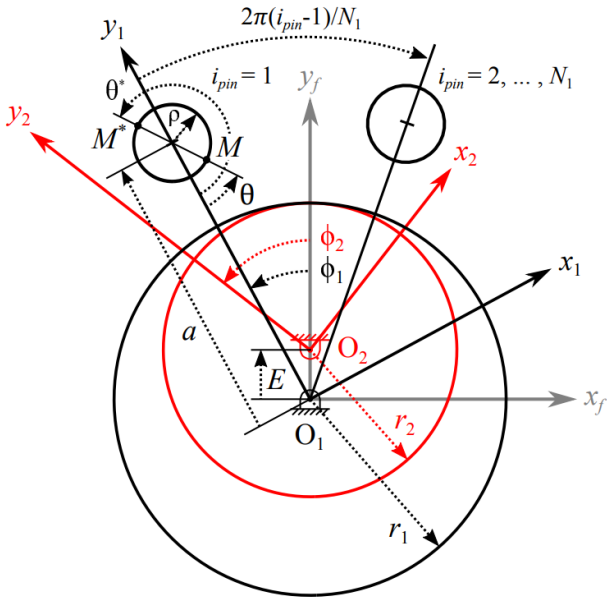

Figure 1: Overcentrode extended epicycloid profile generation (i.e. $m_{21} > 1$ and the pin profile forms part of Ψ_1) showing possible contact points on inner (M) and outer (M^*) pin flanks

When considering the generation of rotor profiles, an important parameter is the gearing ratio, $m_{21} = \omega_2/\omega_1 = N_1/N_2$. Extended epicycloid and hypocycloid profiles can both be generated using this method when $m_{21} > 1$ (as shown in Figure 1) or $m_{21} < 1$ respectively. The extended epicycloidal gearing profile with $m_{21} > 1$ and contact on the inner flank of the pin is often used for gerotor pumps, and is considered here as the basis for investigating the characteristics of asymmetric profiles. Examples of possible profiles are shown in Figure 3; these profiles are defined by the lobe number N_1, the non-dimensional geometric parameters $\lambda = a/r_1$ and $\sigma = \rho/r_1$, and the axis spacing distance $E = r_1/N_1$. The maximum diameter of the outer rotor profile, D, can be determined by considering that, in all cases, the maximum diameter of the inner rotor occurs when $\varphi_1 = \pi$ and $\theta = 0$; once the inner rotor has turned a further half revolution, the tip of the inner and root of the outer rotors must be coincident for a conjugate fillet profile, leading to the definitions in Equation 1.

$$\frac{E}{D} = \frac{1}{2N_1(\lambda - \sigma) + 4}, \quad \frac{a}{D} = \lambda N_1\left(\frac{E}{D}\right), \quad \frac{\rho}{D} = \sigma N_1\left(\frac{E}{D}\right) \tag{1}$$

2.1 Design Envelope of Symmetric Rotors

It can be shown that there are constraints on the values of λ and σ in order to ensure that the pin does not undercut the profiles (Vecchiato et al., 2001). This results in a design envelope for the rotors with particular values of N_1, as shown in Figure 2.

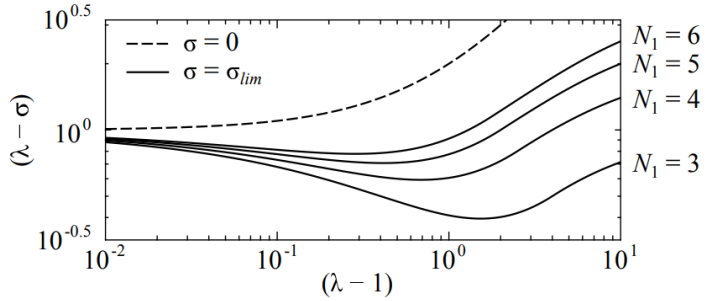

Figure 2: Illustration of how the maximum and minimum possible values of σ as a function of N_1 and λ allow the design envelope of symmetric rotor profiles to be defined.

For the case when $N_1 = 5$, a range of profiles with and without undercutting are illustrated in Figure 3.

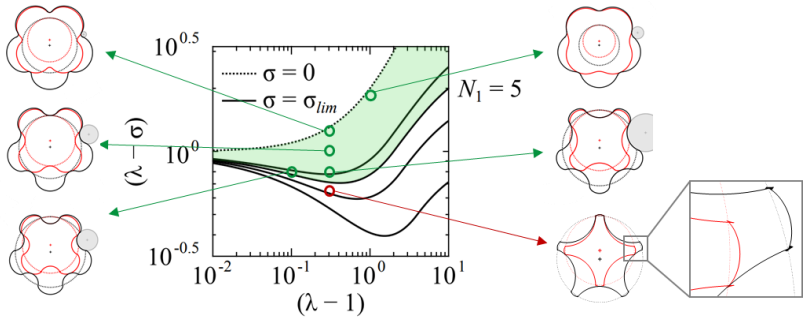

Figure 3: Examples of pin-generated rotor profiles with $N_1 = 5$. Note that undercutting can be seen on the profile that falls outside the design envelope (region shaded green)

2.2 Influence of Rotor Profile on Swept Area

Using conjugate rotor profiles, the area created within the rotors per revolution can be normalized by the total area swept by the tip of the outer rotor profile as shown in Equation 2.

$$\bar{A}_{sw} = \frac{4}{\pi D^2} N_2 A_{wc,max} \tag{2}$$

In the case of a gerotor pump with straight rotors, this normalized swept area for the machine can be used to define the swept volume of the machine, as $V_{sw} = (\pi/4)\bar{A}_{sw} L D^2$. For helical machines, integration is necessary to calculate the volume created per revolution for a given rotor wrap angle. In either case, the value of $\bar{A}_{sw}$ is a useful indicator of machine size required to achieve a given flow rate; in general, the higher the value of $\bar{A}_{sw}$ the more compact the machine, which is likely to lead to other benefits such a reduced leakage flow areas.

The normalised swept area can therefore be calculated as a function of only the rotor profile. The design envelope for different values of lobe number are shown in Figure 4 with corresponding contour plots of the normalised swept area, showing how this tends to decrease with increasing values of N_1 and $(\lambda - \sigma)$.

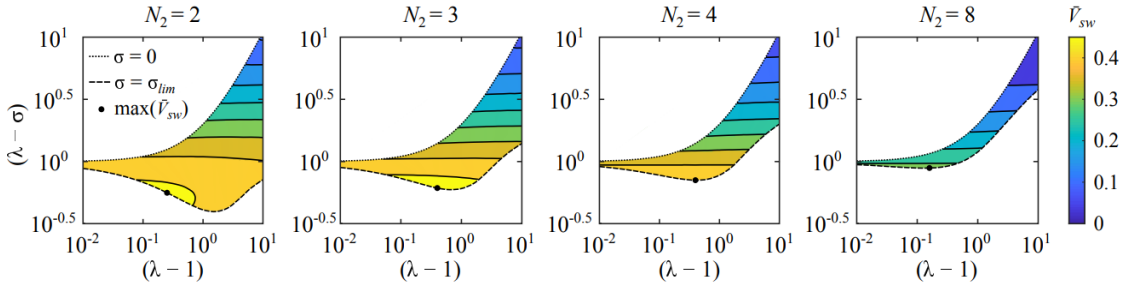

Figure 4: Normalised swept area per revolution of inner rotor for symmetric rotor profiles as function of λ and $(\lambda - \sigma)$ for specified values of N_1

2.3 Profile depth

An important rotor profile parameter influencing performance is the depth of the outer rotor profile relative to the maximum radius. Using the relationships in Equation 1, the proportional profile depth, δ_p, can be defined as shown in Equation 3.

$$\delta_p = \frac{2(r_{max} - r_{min})}{D} = \frac{2}{N_1(\lambda - \sigma) + 2} = \frac{4E}{D} \tag{3}$$

The value of δ_p is therefore dependent on N_1 and $(\lambda - \sigma)$, as illustrated in Figure 5a. The higher the profile depth the larger the radial spacing between the inner and outer rotor profiles at the location of maximum working chamber area. The calculated values of δ_p and $\bar{A}_{sw}$ for the range of viable values of λ and σ shown in Figure 2 are plotted in Figure 5b. It can be seen that the swept volume is strongly dependent on δ_p and is almost independent of the number of lobes for $N_1 > 3$. Maximising the swept area of a particular machine therefore generally requires use of the lowest viable values of N_1 and $(\lambda - \sigma)$.

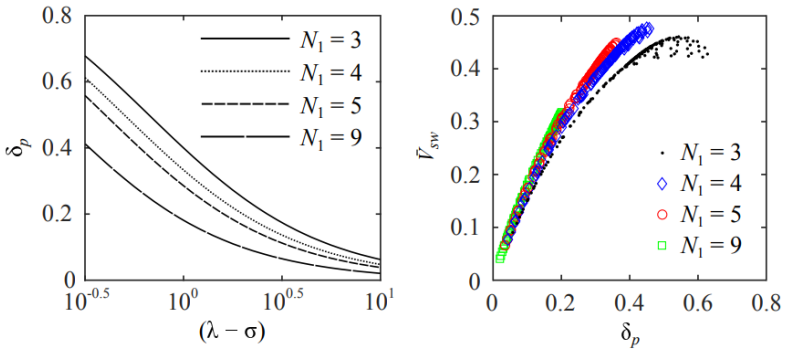

Figure 5: Relative profile depth for the outer rotor as a function of N_1 and$(\lambda - \sigma)$, and the influence on swept area per revolution of the inner rotor, $\bar{A}_{sw}$

3. GEOMETRICAL CHARACTERISTICS OF ASYMMETRIC ROTORS

3.1 Geometrical requirements for asymmetric profiles

Asymmetric circular pin-generated rotor profiles can be created by considering the symmetric profiles created by two circular pins of different diameter and centre location in the coordinate system of the outer rotor, S_1. A viable rotor profile requires the same number of lobes and consistent positions of the rotor axes (i.e. the same value of E). Both pins will generate a pair of conjugate rotors. The inner rotors (Ψ_2) will both have the same axis of rotation. Asymmetric conjugate rotor profiles can then be created by using alternating sections from the intersecting α and β profiles, as illustrated in Figure 6.

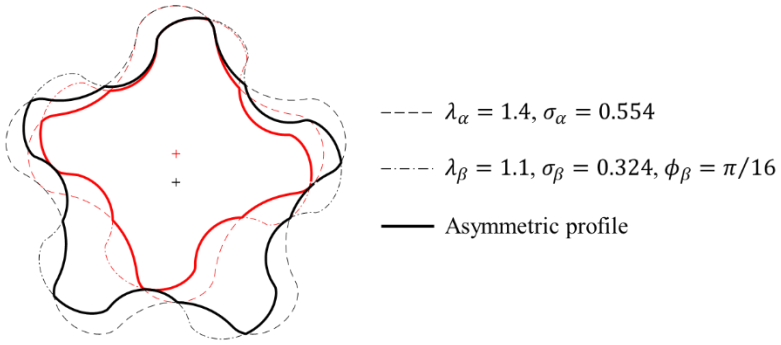

Figure 6: Example of general case of asymmetric rotor profile formed from pins with different values of a and ρ, but with the same value of E

In the general case illustrate in Figure 6, this will cause discontinuities in the gradient of the asymmetric profiles, resulting in points of infinite curvature on both inner and outer rotors. This is avoided in the special case where $\phi_\beta = 0$ and $D_\beta = D_\alpha$. A simple asymmetric configuration can be defined based on two rotor profiles generated with equal values of E, D and δ_p; these profiles will have the same minimum and maximum radii, and an asymmetric profile consisting of alternating half-lobes of the two symmetric profiles can therefore be created. This is equivalent to a profile generated using the asymmetric pin geometry illustrated in Figure 7. Equation 1 shows that this is only possible if the value of $(\lambda - \sigma)$ is constant; $(a - \rho)$ must therefore be the same for both pin sections if D is fixed.

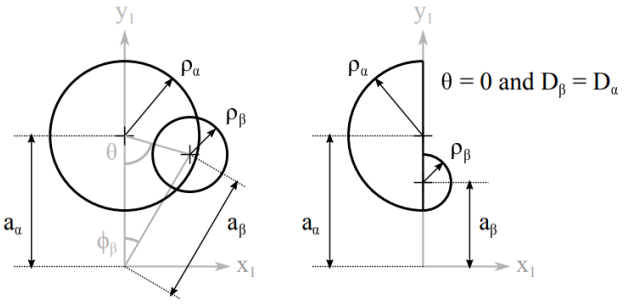

Figure 7: Example of the 2-pin geometry used to generate asymmetric rotor profiles; a) general case and b) simple case where $(a_\alpha - \rho_\alpha) = (a_\beta - \rho_\beta)$.

As with conventional symmetric gerotor profiles, the same constraints apply to the two different combinations of λ and σ values that define the asymmetric profile in order to ensure that no undercutting occurs. The design envelopes shown in Figure 4 therefore also define the limiting conditions for viable asymmetric profiles, as illustrated in Figure 8. An asymmetric profile can be generated by selecting any two values of λ that satisfy the condition of constant $(\lambda - \sigma)$ and that lie between the limits of $0 \leq \sigma \leq \sigma_{lim}$; examples of this are shown in Figure 9 for a case with $N_1 = 5$ and $(\lambda - \sigma) = 0.775$.

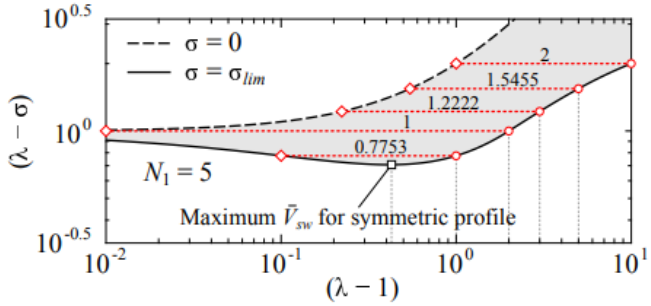

Figure 8: Example of the design envelope for asymmetric profiles with $N_1 = 5$, showing the range of possible λ values for constant $(\lambda - \sigma)$ values corresponding to $\lambda_{max} = 2, 3, 4, 6$ and 11. Note that the maximum value of $\bar{A}_{sw}$ for a symmetric profile is achieved with $\bar{\sigma} = 1$ (i.e. $\sigma = \sigma_{lim}$) and $\lambda = 1.42$

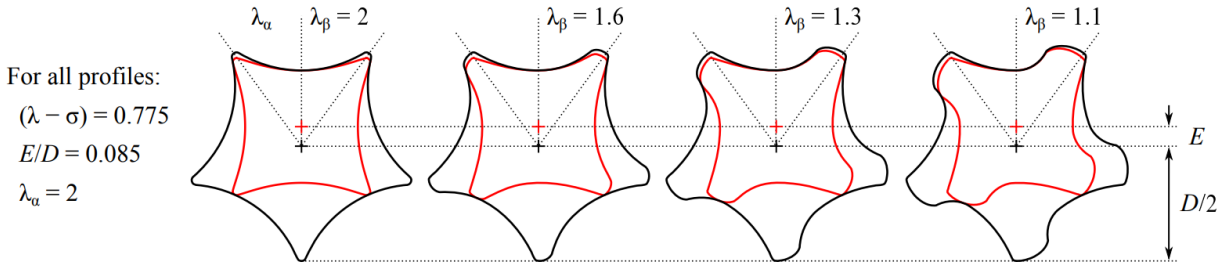

Figure 9: Examples of asymmetric pin-generated rotor profiles with $N_1 = 5$ and $(\lambda - \sigma) = 0.775$. All profiles are shown with the same value of D

It is clear from the examples shown in Figure 9 that this method can produce asymmetric rotor profiles that avoid points of infinite curvature likely to results in high contact stress and wear. The rotor profile can now be characterised using the parameters $N_1, \lambda_\alpha, \bar{\sigma}_\alpha$ and λ_β; hence the use of asymmetric rotors provides an additional geometrical parameter that can be used to optimise the performance of a machine.

3.2 Influence of Asymmetric Profile on Swept Area

The area of the working chamber formed between the rotors for asymmetric profiles can be found as for the conventional symmetric profiles. This is illustrated in Figure 10, which shows the normalised swept area calculated for a range of asymmetric profiles with $N_1 = 5$ and $(\lambda - \sigma) = 1$. Results are shown for three different cases:

i. The rotor profile is symmetrical, hence $\lambda_\alpha = \lambda_\beta$
ii. $\lambda_\alpha = 1.01$ (i.e. the minimum possible value as shown in Figure 8)
iii. $\lambda_\alpha = 3$ (i.e. the maximum possible value as shown in Figure 8)

In each case, the normalised swept area is then calculated for the range $1.01 \leq \lambda_\beta \leq 3$.

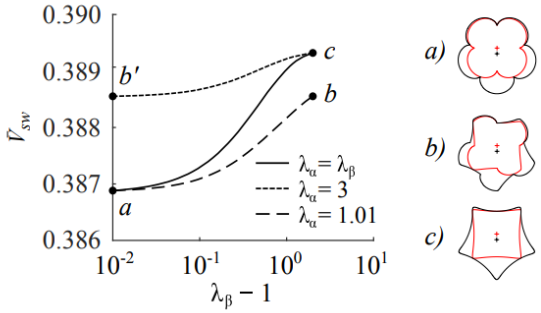

Figure 10: Normalised swept area for symmetric and asymmetric rotor profiles as function of λ for $(\lambda - \sigma) = 1$ and $N_1 = 5$. Note that the profile for point b' is the mirror image of b.

Based on this analysis, there are two important points to note:

- For symmetric profiles, Figure 4 shows that the normalised swept area, $\bar{A}_{sw}$, depends strongly on $(\lambda - \sigma)$. As this must be constant for the asymmetric profiles, it is apparent that asymmetric profiles will have similar values of $\bar{A}_{sw}$ to these symmetric cases. This is demonstrated by the example in Figure 10, which illustrates the second order influence of λ values on $\bar{V}_{sw}$ for both symmetric and asymmetric profiles.
- For values of $N_1 > 4$ the maximum values of $\bar{A}_{sw}$ is achieved with the minimum possible value of $(\lambda - \sigma)$. As asymmetric profiles can only be achieved with a higher value of $(\lambda - \sigma)$, they must therefore achieve a lower $\bar{A}_{sw}$ than the maximum possible value.

This analysis suggests that the use of asymmetric pin-generated gerotor profiles does not offer significant benefits in terms of the swept volume for machines with either straight or helical rotors. Consideration of other factors relating to performance is necessary as discussed below.

3.4 Influence on Port Areas

Asymmetric rotor profiles result in different working chamber geometry during the periods of increasing and decreasing volume. The curve of volume as a function of rotor position is therefore no longer symmetric, and the location of maximum volume needs to be identified. The ports must also be shaped in order to match the asymmetric profiles. As for conventional symmetric profiles, these can be defined in order to maximise the flow area in or out of the working chamber, while still opening and closing at the required positions (generally corresponding to maximum and minimum volume). The working chamber area and the port areas for a gerotor pump configuration (i.e. with non-helical rotors) are shown for specified symmetric and asymmetric rotor profiles in Figure 11.

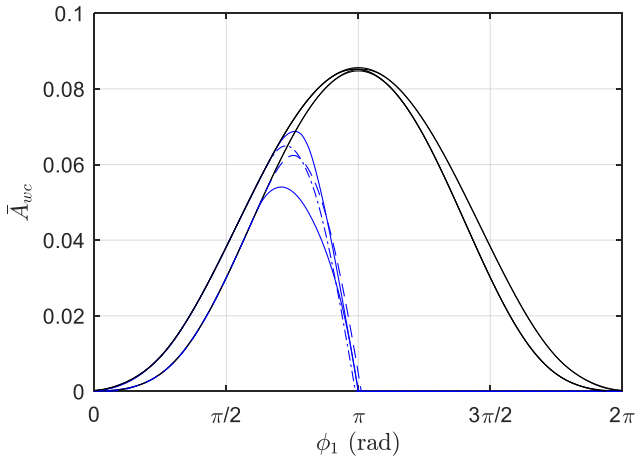

Figure 11: Working chamber area (black lines) and inlet port area (blue lines) for symmetric (solid lines; $\lambda = 1.1$, $\lambda = 2$) and asymmetric (dashed lines; $\lambda_\alpha = 1.1$ & $\lambda_\beta = 2$, and vice versa) rotor profiles with $N_1 = 5$ and $(\lambda - \sigma) = 0.775$

The results in Figure 11 show that asymmetric profiles affect both the flow area and the rate of change of working chamber volume. The pressure drop during filling will therefore be affected; more detailed modelling of the fluid filling process is needed to understand the influence of this on the machine performance.

3.3 Influence on Rotor Torques

Asymmetric profiles change the relative positions of the contact points between the inner and outer rotors. This modifies both the projected area for the pressure force to act on each rotor, and the torque arm that occurs between the resultant force and each axis of rotation. This is illustrated in Figure 12, which shows a single cycle of the net torque acting on the inner and outer rotors during operation, assuming constant pressure during filling and discharge with a fixed pressure difference, Δp; the rotor profiles are the same as those considered in Figure 11, and the asymmetric profiles are seen to combine characteristics of the two symmetric profiles.

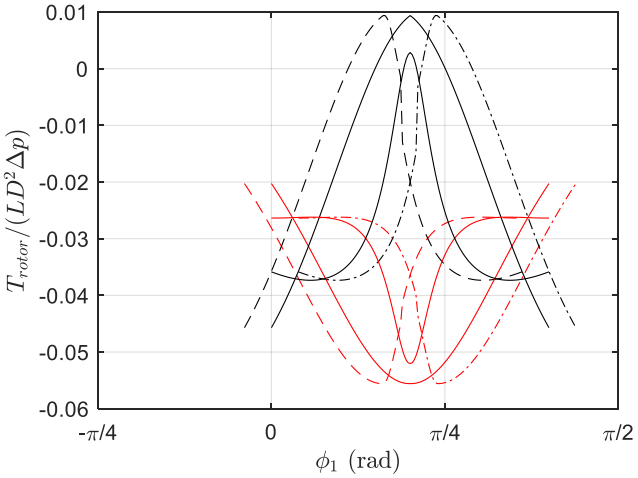

Figure 12: Influence of rotor profile on the net rotor torque for the symmetric (solid lines) and asymmetric (dashed lines) profiles shown in Figure 11

Furthermore, asymmetric profiles affect the curvature of the rotors at the contact point. Both the rotor torque and the geometry of the rotors at the contact point will vary with rotor position, and need to be considered in order to assess the influence of asymmetric profiles on the contact stresses that occur in the rotors during operation.

6. CONCLUSIONS

The current study has shown that asymmetric gerotor profiles can be defined and generated using the same principles and design envelopes as for conventional symmetric pin-generated profiles. The proposed profiles maintain finite curvature at all points by combing sections of two rotor profiles with equal values of N_1, E and D. The profile depth of the asymmetric profiles is therefore the same as either of the constituent symmetric profiles, hence the normalised swept area is found to be similar.

The use of asymmetric profiles has also been shown to affect both the filling process for the machine (via the influence on rate of change of volume, and port area), and the contact stress and wear that occurs during operation (via the net rotor torque and the relative curvature at the contact points). A more detailed analysis of the operation of gerotor machines is therefore necessary in order to fully assess whether this type of asymmetric profile offers any significant benefits when optimised for a particular pump or compressor application.

NOMENCLATURE

L	Rotor length	(m)
V	Volume	(m^3)
r	Centrode radius	(m)
A	Area	(m^2)
D	Max rotor profile diameter	(m)
a	Radial distance to pin centre	(m)
ρ	Radius of pin	(m)
E	Distance between rotor axes	(m)
N	Number of lobes on rotor	(-)
θ	Profile pin contact angle	(rad)
Ψ	Rotor profile	(-)
λ	Normalised radial distance to pin centre	(-)
σ	Normalised radius of pin	(-)

Subscript

$1, 2$	Outer or inner rotor
wc	Working chamber
sw	Swept area or volume
α, β	Generating pin section for asymmetric profile

REFERENCES

Beard, J., Hall, A., and Soedel, W. (1991). "Comparison of hypotrochoidal and epitrochoidal gerotors". Journal of Mechanical Design, 113, pp. 133–141.

Beard, J. E., Yannitell, D. W., & Pennock, G. R. (1992). The effects of the generating pin size and placement on the curvature and displacement of epitrochoidal gerotors. Mechanism and Machine Theory, 27(4), 373-389.

Colbourne, J. (1974). "The geometry of trochoid envelopes and their application in rotary pumps". Mechanism and Machine Theory, 9(3).

De Martin, A., Jacazio, G., & Sorli, M. (2019). Optimization of gerotor pumps with asymmetric profiles through an evolutionary strategy algorithm. Machines, 7(1), 17.

Hsieh, C., and Hwang, Y. (2007). "Geometric design for a gerotor pump with high area efficiency". Journal of Mechanical Design, 129(12), pp. 1269–1277.

Hsieh, C. (2009). "Influence of gerotor performance in varied geometrical design parameters". Journal of Mechanical Design, 131(12), p. 121008.

Hsieh, C. (2012). "Fluid and dynamics analyses of a gerotor pump using various span angle designs". Journal of Mechanical Design, 134(12), p. 121003

Litvin, F., and Feng, P. (1996). "Computerized design and generation of cycloidal gearings". Mechanism and Machine Theory, 31(7), pp. 891–911.

Moineau, R. (1934). "Gear mechanism". U.S. Patent 1,892,217.

Read, M. G., Stosic, N. and Smith, I. K. (2020). The influence of rotor geometry on power transfer between rotors in gerotor-type screw compressors. Journal of Mechanical Design, 142(7)

Read, M. G., Smith, I. K., & Stosic, N. (2022). Influence of rotor geometry on tip leakage and port flow areas in gerotor-type twin screw compressors. Proceedings of the Institution of Mechanical Engineers, Part E: Journal of Process Mechanical Engineering, 236(1), 94-102.

Rundo, M. (2017). "Models for flow rate simulation in gear pumps: A review". Energies, 10(9), p. 1261.

Vecchiato, D., Demenego, A., Argyris, J., and Litvin, F. (2001). "Geometry of a cycloidal pump". Computer methods in applied mechanics and engineering, 190(18), pp. 2309–2330